

Optical response of dipole antennas on an epsilon-near-zero substrate

Sebastian A. Schulz,¹ Asad A. Tahir,¹ M. Zahirul Alam,¹ Jeremy Upham,¹ Israel De Leon,^{1,2,*} and Robert W. Boyd^{1,3}

¹*Department of Physics and Max Planck Centre for Extreme and Quantum Photonics, University of Ottawa, 25 Templeton Street, Ottawa, K1N 6N5, Canada*

²*School of Engineering and Sciences, Tecnológico de Monterrey, Monterrey, Nuevo León 64849, Mexico*

³*Institute of Optics and Department of Physics and Astronomy, University of Rochester, 275 Hutchison Road, Rochester, New York 14627, USA*

(Received 11 March 2016; published 27 June 2016)

Materials with vanishing permittivity (epsilon-near-zero or ENZ materials) show unconventional optical behavior. Here we show that plasmonic dipole antennas on an ultrathin ENZ substrate have properties significantly different from antennas on a traditional substrate. Specifically, the presence of a 23-nm-thick ENZ material strongly modifies the linear response of plasmonic antennas and, as a result, the resonant wavelength is independent of the linear dimensions of the dipole antenna.

DOI: [10.1103/PhysRevA.93.063846](https://doi.org/10.1103/PhysRevA.93.063846)

I. INTRODUCTION

The epsilon-near-zero (ENZ) property of materials, both naturally occurring or artificial metamaterials, promises new avenues for optics [1,2]. In the ENZ range of the spectrum the real part of the permittivity, ϵ , approaches or crosses zero while the imaginary part usually remains finite. The near-zero response can be obtained in various material systems, including highly doped semiconductors [3], metal-dielectric composite structures [4], or in integrated optical platforms [5,6]. Materials that possess an ENZ spectral region exhibit many unusual optical properties, including nearly arbitrary control of light propagation [7–11] and the wielding of diverse nonlinear phenomena [12–14]. One particular area of interest is the effect of this vanishing permittivity on nearby optical structures [8,9,15–17].

Recently there has been a tremendous interest in designing metasurfaces with tailored electromagnetic properties [18–20]. In this letter we discuss the impact of an ultrathin ENZ substrate on the optical behavior of plasmonic antenna arrays that are designed for operation near the ENZ spectral region. We choose the array dimensions such that there is no near-field coupling between the dipole antennas. We find that in such a hybrid plasmonic-ENZ system strong coupling occurs between the antenna resonance and modes within the ENZ layer. Consequently, the resonance is split, with the resonance wavelength independent of variations in the antenna dimensions. We further investigate the field distribution within the hybrid ENZ-antenna system.

II. CONSTITUENT COMPONENTS

The ENZ material employed for our study is a thin layer of indium tin oxide (ITO), a degenerate semiconductor that exhibits a vanishing real part of the permittivity in the near-infrared spectral region. The ITO was obtained from a commercial supplier and consists of a 23-nm-thick ITO film on a 1.1-mm-thick float glass substrate. We determined the permittivity of the ITO layer over a broad wavelength range through spectroscopic ellipsometry, with the results shown in

Fig. 1. We observe that the real part of the permittivity, ϵ , is zero at $\lambda_0 = 1417$ nm and remains between 1 and -1 for the spectral region spanning from 1200 nm to 1600 nm.

Thin ENZ material layers, such as the one employed here, support optical modes with a large local density of states [21]. We obtain the dispersion curve of our bare ITO-glass substrate by computing the local minima of the substrate's reflectance spectrum using the Nelder-Mead method. The generated dispersion diagram is shown in Fig. 1(b), where two modes can be identified: the Brewster mode and the Ferrell-Berremann mode [21–23]. The Ferrell-Berremann mode has a high density of states [21], as demonstrated by its shallow slope. Since this mode is formed in a film that is thinner than the skin depth in ITO, the transverse field is expected to be constant throughout the film when it is excited [24]. The portion of the Ferrell-Berremann mode below the light line is sometimes also referred to as the ENZ mode. We note that the modes in the ITO layer are not excited under normal incidence illumination. Such illumination results in a monotonically decreasing transmission with increasing wavelength (the transmission drops from 94% to 78%), due to the increased absorption in the ITO layer, see green curve in Fig. 1(a).

Due to its large density of states, the Ferrell-Berremann mode can significantly alter the properties of nearby optical scatterers. To study this phenomenon, we fabricated multiple arrays of gold antennas on the ITO substrate [see Fig. 2(a)]. The antennas were designed to have their fundamental resonance near the ENZ spectral region of the ITO film, in the absence of the ITO layer, as shown in Fig. 2(b). Each array has a square lattice with a fixed period of 600 nm. All antennas have a length of 404 ± 8 nm and their width varies across the arrays, from 37 nm to 77 nm. These dimensions were confirmed through scanning electron microscopy (SEM) measurements. Fabrication was performed according to the recipe in Ref. [20], using a Raith Pioneer electron-beam lithography system, followed by gold evaporation and liftoff.

It is well known that a dipole antenna has a single optical resonance, for light polarized parallel to the antenna length. This resonance is strongly dependent on the dimensions, both length and width, of the antenna [25,26]. Figure 2(b) shows how the resonance wavelength, obtained from finite-difference-time-domain (FDTD) simulations, shifts for dipole antennas of the various dimensions used in our experiment, but

*ideleon@itesm.mx

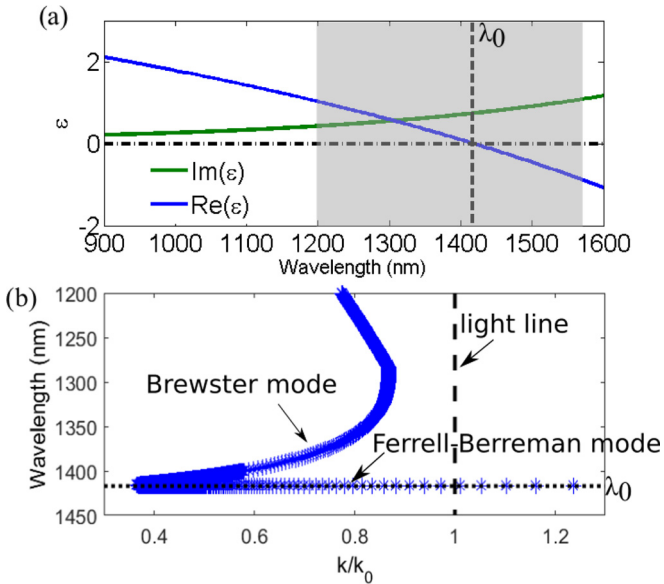


FIG. 1. (a) Experimentally obtained permittivity for the 23-nm-thick ITO layer. The real part of ϵ crosses zero at 1417 nm. The gray shading indicates the region of the spectrum where $-1 \leq \epsilon \leq 1$. (b) Dispersion relation for the modes supported by the 23-nm-thick ITO layer on a glass substrate. The black dotted and dashed lines represent the wavelength at which $\text{Re}(\epsilon) = 0$ (λ_0) and the air (top cladding) light line, respectively. k_0 is the free space wave vector. The plot shows that the Ferrell-Berremann mode has a high density of states, indicated by the shallow slope in this plot, near λ_0 .

on a simple glass substrate without the ENZ layer. It is clearly visible that the resonance wavelength is strongly dependent on the geometric parameters; in this case, reducing the width from 77 nm to 37 nm results in a redshift of over 200 nm.

III. CHARACTERIZATION

For our experimental study, we measured the transmission of light (normalized to transmission through the bare ITO film on glass) from a tungsten halogen source through the sample and detected the transmitted light using an optical spectrum analyzer. A polarizer was used to select only the polarization of light parallel to the antenna. Our measurements, shown in Fig. 2(c), reveal that there is a strong resonance in the region of $1320 \text{ nm} \leq \lambda \leq 1380 \text{ nm}$ for all arrays. However, we observe that the resonance of the dipole antennas on ITO is almost independent of the antenna dimensions. This is in contrast to the behavior of an identical set of antenna arrays on glass (without ITO) simulated earlier, which exhibit a redshift of the resonance wavelength that exceeds 200 nm. In the combined system, the main impact of changing the antenna dimension is a change of the extinction ratio, from a 30% to a 45% dip in the on-resonance transmission. Furthermore, while the antennas on glass have a symmetric resonance, the combined system has a strongly asymmetric spectral behavior, with suppressed transmission on the long-wavelength edge of the resonance. A similar behavior can be observed in FDTD simulations of the dipole antennas on our ENZ substrate [dashed lines in Fig. 2(c)]. The observation of an asymmetric resonance, with the resonant wavelength being independent of

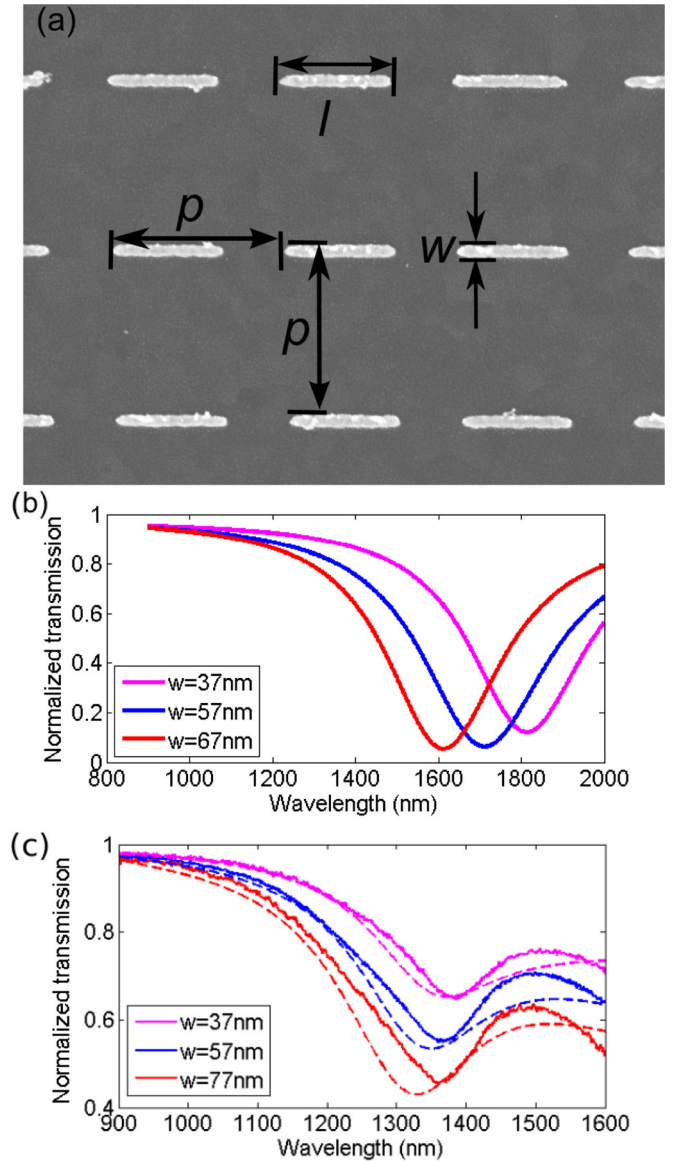


FIG. 2. (a) Scanning electron microscope image of an antenna array outlining the design parameters length l , width w , and period p . The period corresponds to 600 nm. (b) Simulated transmission spectra of three arrays of dipole antennas on glass, without the ENZ substrate. The resonance wavelength is redshifted as w is decreased at constant l . The simulated antennas have a periodicity of 600 nm, a length of 404 ± 8 nm, and a width of 37 nm (magenta/light gray), 57 nm (blue/dark gray), and 77 nm (red/medium gray), respectively, matching the dimensions of the antennas fabricated on the ENZ substrate. (c) Experimental (solid lines) and simulated (dashed lines) transmission curves for three antenna arrays, with the same dimensions as panel (b). All transmission curves are normalized to the transmission through a bare ITO film on glass.

the antenna dimensions, is a remarkable consequence of the strong interaction between the optical modes of the plasmonic antenna and those of the thin ENZ layer.

IV. DISCUSSION

We now discuss the physics underlying the observed optical behavior. From Fig. 2(c) we note that the resonance spectra

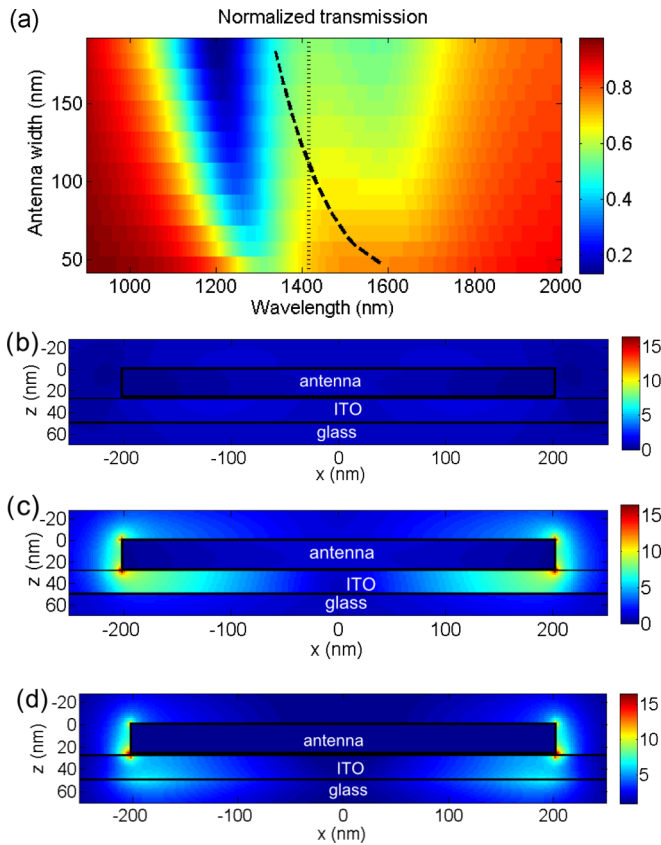


FIG. 3. (a) Evolution of the combined dipole antenna-ENZ substrate resonance with varying antenna width. The color indicates the simulated transmission through the system. The dotted and dashed lines indicate the Ferrell-Berreman mode, at λ_0 , and the resonance wavelength of the same dipole antennas on a glass substrate, respectively. (b–d) Electric field strength plots, along the antenna cross section, for an antenna with a length of 400 nm and a width of 57 nm. The color indicates the field strength, normalized to the incident light. (b) At $\lambda = 1.0 \mu\text{m}$, away from the antenna resonance and outside the ENZ region. (c) At $\lambda = 1.35 \mu\text{m}$, in the ENZ region and at the observed resonance. (d) At $\lambda = 1.67 \mu\text{m}$, centered on the second resonance dip, close to the resonance wavelength of the antenna in the absence of the ENZ layer.

are characterized by two transmission dips, one occurring for wavelength slightly shorter than λ_0 and the second occurring for wavelengths above 1550 nm; for the most part these wavelengths were inaccessible in our experiment, due to limitations on the detection bandwidth. These spectra exhibit a strong splitting of the antenna's dipole resonance, occurring near λ_0 , where the ITO film supports the Ferrell-Berreman mode. To investigate this behavior further, we performed FDTD simulations of a larger range of antenna dimensions and over a larger wavelength range, mapping the evolution of the combined ENZ-dipole antenna system. We also calculate the field distribution of the excited modes. Figure 3(a) shows the evolution of the resonance as the antenna width is increased. Note that the antenna length was reduced to 350 nm for these simulations to achieve a better spectral overlap of the antenna resonance and the ENZ spectral region. We see that the system has two resonances, with both an increasing extinction and increasing separation between the

resonances as the antenna width increases. Increasing the antenna width results in stronger coupling between the ENZ layer and the antenna resonance, as an increased width leads to a blueshift of the antenna resonance wavelength. Therefore we attribute the observed behavior to a strong coupling between the Ferrell-Berreman mode of the ITO film and the antenna resonance, consistent with recent observations by Campione *et al.* [17], where a dependence of the splitting on the ITO film thickness was demonstrated. A similar splitting is not observed for the case of thick ITO films [27], which do not support the Ferrell-Berreman mode.

We now further investigate the nature of the observed resonances. We can separate the transmission spectra into three distinct regions: short wavelengths, below both resonances; near the shorter wavelength resonance; and near the longer wavelength resonance. The first spectral region is away from either resonance and outside of the ENZ region. Here, the light only weakly interacts with the dipole antenna and the ENZ layer, and consequently, strong transmission is observed. This is confirmed by the lack of field enhancement observed in the cross section shown in Fig. 3(b). As the wavelength is increased we enter the second and third spectral regions, where the two resonances are located. Figures 3(c) and 3(d) show the field distributions for the two resonances. At the shorter wavelength resonance, the field is enhanced on the antenna and in the ENZ layer. Except at the termination of the antenna, the field distribution within the ITO layer shows the main hallmarks of the Ferrell-Berreman mode, i.e., a weak z dependence within this layer and an abrupt termination at the ITO-glass interface [24]. Since the ENZ wavelength is independent of the antenna dimensions, the resonance wavelength associated with this mode is constant for all arrays. However, antennas in different arrays have different scattering cross sections and a different resonance wavelengths. Therefore, they have varying interaction strengths with the incident light in this wavelength region and different coupling strengths with the Ferrell-Berreman mode, resulting in the different transmission values observed in Figs. 2(c) and 3(a). We note that in this wavelength range the electric field in the ENZ medium is significantly enhanced [see Fig. 3(c)]. For example, ignoring the hot spots formed at the sharp edges of the antenna, we obtain a six- to eightfold field enhancement in the ENZ medium, corresponding to an enhancement of the field intensity of approximately 50. From Fig. 3(d) we observe that the field distribution associated with this second, longer wavelength resonance has two separate regions with field enhancement, near the antenna and at the ITO-glass interface. In this wavelength region the ITO layer does not support the Ferrell-Berreman mode anymore but supports a leaky surface mode confined to the ITO-air interface. This mode is heavily damped by radiative and material losses. Therefore the field is confined tightly to the dipole antenna, has a z -dependent field distribution within the ITO layer, and shows a modest field enhancement at the ITO-glass boundary, associated with a weak coupling to the surface plasmon modes.

V. CONCLUSION

We have shown that the presence of a thin ENZ substrate strongly affects the optical response of antenna arrays

operating in the ENZ spectral region through a strong coupling between the Ferrell-Berreman mode in the ENZ substrate and the antenna resonance. Far away from the antenna resonance and outside of the ENZ region, light is only weakly affected by the system, while closer to the wavelength where $\text{Re}(\epsilon) = 0$ the Ferrell-Berreman mode and the fundamental resonance of the dipole antenna strongly couple, leading to a splitting of the antenna resonance into two new resonances. In addition, our optical field analysis shows that these two resonances have very different optical behavior. On one resonance the field is enhanced both on the antenna and within the ITO layer, where the Ferrell-Berreman mode is excited. On the other resonance,

the field enhancement is limited to regions near the dipole antenna, with weak coupling to lossy surface plasmon modes at the ITO-glass boundary. Our work provides a simple model describing the optical behavior of dipole antenna arrays on thin ENZ substrates and paves the way toward uses of such structures, for example, for further enhancement of the already strong nonlinear response of ENZ systems [3,10].

ACKNOWLEDGMENTS

We gratefully acknowledge the support of the Canada Excellence Research Chair (CERC) program and from NSERC.

-
- [1] N. Engheta, *Science* **340**, 286 (2013).
- [2] A. Alù, M. G. Silveirinha, A. Salandrino, and N. Engheta, *Phys. Rev. B* **75**, 155410 (2007).
- [3] M. Z. Alam, I. D. Leon, and R. W. Boyd, *Science* **352**, 795 (2016).
- [4] S. Molesky, C. Dewalt, and Z. Jacob, *Opt. Express* **21**, A96 (2013).
- [5] R. Maas, J. Parsons, N. Engheta, and A. Polman, *Nat. Photonics* **7**, 907 (2013).
- [6] Y. Li, S. Kita, P. Muñoz, O. Reshef, D. I. Vulis, M. Yin, M. Lončar, and E. Mazur, *Nat. Photonics* **9**, 738 (2015).
- [7] M. A. Vincenti, D. de Ceglia, A. Ciattoni, and M. Scalora, *Phys. Rev. A* **84**, 063826 (2011).
- [8] C. Argyropoulos, P.-Y. Chen, G. D'Aguanno, N. Engheta, and A. Alù, *Phys. Rev. B* **85**, 045129 (2012).
- [9] H. Aouani, M. Rahmani, M. Navarro-Cía, and S. a. Maier, *Nat. Nanotechnol.* **9**, 290 (2014).
- [10] A. Capretti, Y. Wang, N. Engheta, and L. D. Negro, *Opt. Lett.* **40**, 1500 (2015).
- [11] T. S. Luk, D. de Ceglia, S. Liu, G. A. Keeler, R. P. Prasankumar, M. A. Vincenti, M. Scalora, M. B. Sinclair, and S. Campione, *Appl. Phys. Lett.* **106**, 151103 (2015).
- [12] R. Liu, Q. Cheng, T. Hand, J. J. Mock, T. J. Cui, S. A. Cummer, and D. R. Smith, *Phys. Rev. Lett.* **100**, 023903 (2008).
- [13] D. C. Adams, S. Inampudi, T. Ribaudo, D. Slocum, S. Vangala, N. A. Kuhta, W. D. Goodhue, V. A. Podolskiy, and D. Wasserman, *Phys. Rev. Lett.* **107**, 133901 (2011).
- [14] S. Savoia, G. Castaldi, V. Galdi, A. Alù, and N. Engheta, *Phys. Rev. B* **91**, 115114 (2015).
- [15] Y. C. Jun, J. Reno, T. Ribaudo, E. Shaner, J.-J. Greffet, S. Vassant, F. Marquier, M. Sinclair, and I. Brener, *Nano Lett.* **13**, 5391 (2013).
- [16] T. Galfsky, Z. Sun, Z. Jacob, and V. M. Menon, *Opt. Mater. Express* **5**, 2878 (2015).
- [17] S. Campione, J. R. Wendt, G. A. Keeler, and T. S. Luk, *ACS Photonics* **3**, 293 (2016).
- [18] N. Yu and F. Capasso, *Nat. Mater.* **13**, 139 (2014).
- [19] D. Lin, P. Fan, E. Hasman, and M. L. Brongersma, *Science* **345**, 298 (2014).
- [20] S. A. Schulz, J. Upham, F. Bouchard, I. D. Leon, E. Karimi, and R. W. Boyd, *Opt. Mater. Express* **5**, 2798 (2015).
- [21] S. Vassant, J.-P. Hugonin, F. Marquier, and J.-J. Greffet, *Opt. Express* **20**, 23971 (2012).
- [22] T. Taliercio, V. N. Guilengui, L. Cerutti, E. Tourine, and J.-J. Greffet, *Opt. Express* **22**, 24294 (2014).
- [23] W. D. Newman, C. L. Cortes, J. Atkinson, S. Pramanik, R. G. D. Corby, and Z. Jacob, *ACS Photonics* **2**, 2 (2015).
- [24] S. Campione, I. Brener, and F. Marquier, *Phys. Rev. B* **91**, 121408 (2015).
- [25] L. Novotny, *Phys. Rev. Lett.* **98**, 266802 (2007).
- [26] G. W. Bryant, F. J. Garcia de Abajo, and J. Azipurua, *Nano Lett.* **8**, 631 (2008).
- [27] J. Kim, A. Dutta, G. V. Naik, A. J. Giles, F. J. Bezares, C. T. Ellis, J. G. Tischler, A. M. Mahmoud, H. Caglayan, O. J. Glembocki, A. V. Kildishev, J. D. Caldwell, A. Boltasseva, and N. Engheta, *Optica* **3**, 339 (2016).